

SCIENTIFIC REPORTS



OPEN

Designation of highly efficient catalysts for one pot conversion of glycerol to lactic acid

Meilin Tao¹, Dan Zhang¹, Hongyu Guan¹, Guohui Huang² & Xiaohong Wang¹

Received: 22 April 2016

Accepted: 24 June 2016

Published: 19 July 2016

Production of lactic acid from glycerol is a cascade catalytic procedure using multifunctional catalysts combined with oxidative and acidic catalytic sites. Therefore, a series of silver-exchanged phosphomolybdic acid catalysts ($\text{Ag}_x\text{H}_{3-x}\text{PMo}_{12}\text{O}_{40}$, $x = 1 \sim 3$, abbreviated as Ag_xPMo) was designed and applied in glycerol oxidation with O_2 as an oxidant to produce lactic acid (LA) without adding any base. Among all, total silver exchanged phosphomolybdic acid (Ag_3PMo) was found to be the most active one with LA selectivity of 93% at 99% conversion under mild conditions of 5 h at 60 °C. The exceptionally high efficiency was contributed to the generation of strong Lewis acid sites, enhanced redox potentials and water-tolerance. More importantly, Ag_3PMo was tolerant in crude glycerol from biodiesel production. And the reaction mechanism was also discussed. Meanwhile, Ag_3PMo acted as a heterogeneous catalyst for 12 recycles without loss of activity.

Cascade or tandem reactions are often carried out in one pot to maximize spatical and temporal productivity with mobilization of minimum resources¹. From the “Green chemistry” point of view, cascade reactions can increase the economic competitiveness in the production of target compounds by reducing the isolation of synthetic intermediates and unnecessary purifications. The key point in cascade reaction is to create a new catalyst that is active to promote all the individual reactions involved in the cascade reactions^{2–4}. By now, a series of cascade catalysts have been developed including those with acids and bases or redox sites as active centers. To fabricate such multifunctional catalysts, multi-components are usually needed comprising of noble metals Pt, Au, Pd or Ru and acids or bases through loading these metal nanoparticles on probable acid or base supports⁵. Because of the increasing interest for developing cascade reactions in catalysis, other new possible strategies to create higher numbers of catalytic centers are desirable and would open unforeseen avenues in catalysis. In addition, if there is a catalyst with more than two active sites such as acid, base and metal centers, it would be highly useful for direct conversion of bio-derived feedstock into fine chemicals⁶ to avoid forthcoming oil shortage and mitigate global warming. However, it is more difficult in the implementation of bio-derived resources into cascade processes because of rare existence of highly active moieties and numerous side-reactions. Therefore, it becomes clear that the use of new catalysts with more active sites is crucial for facing future challenges.

One of the most important cascade reactions in conversion of bio-based feedstock is the conversion of glycerol to green bulk chemicals^{5,7–9}. Among these, lactic acid (LA) has gained significant interesting, which is considered as a top 12 biobased platform molecule and may serves as a useful precursor and platform chemical for producing polymers and green solvents^{10,11} with wide applications in packaging food, cosmetic, and pharmaceutical industry^{12,13}. In generally, LA is mainly produced (approximately 95% of world production) from sugars and sugar alcohols via the fermentation route at strict temperature (<313 K) and pH 5–7 followed by purification, distillation and hydrolysis, which shows sustainability problems associated with the up-scaling of the current fermentation route and waste disposal¹⁴. Therefore, there is a persistent need to develop efficient methods for production of LA. An alternative production of LA from glycerol generally requires oxidation and then dehydration/rehydration steps to LA under reductive or inert conditions, or with oxidants or electrochemicals. By now, high-yield (80%) hydrothermal conversion of glycerol has been achieved in harsh alkaline conditions at a high temperature (573 K)¹⁵, which was not an economic process. Recently, a cascade reaction has been developed to selectively transform glycerol to LA under oxidative conditions using bio- and chemocatalysts, which is more logical^{16–21}.

¹Key Lab of Polyoxometalate Science of Ministry of Education, Northeast Normal University, Changchun 130024, P. R. China. ²School of Biology, Northeast Normal University, Changchun 130024, People's Republic of China. Correspondence and requests for materials should be addressed to G.H. (email: huanggh699@nenu.edu.cn) or X.W. (email: wangxh665@nenu.edu.cn)

Firstly, glycerol is selectively oxidized to dihydroxyacetone (DHA) and glyceraldehydes (GCA) in the presence of metal catalysts; secondly, GCA and DHA undergo dehydration to pyruvaldehyde (PAL); finally, PAL hydrated or benzilic acid rearranged to LA by base-catalysis. However, GCA and DHA are very prone to be further oxidated to the undesired by-product glyceric acid (GlyA) or tartronic acid. For the reported processes, LA was obtained via aerobic oxidation of glycerol catalyzed by noble-metal catalysts including Au-Pt/TiO₂¹⁶ (85% selectivity at 30% conversion at 90 °C, 4 h), AuPt/CeO₂²² (80% selectivity at 99% conversion at 100 °C for 30 min), Pt₁Ni₁O_x/TiO₂¹⁷ (62.6% selectivity at 99.1% conversion at 90 °C for 2 h), and homogeneous Ir (I) bis-carbonyl complex²⁰ (96% selectivity at 94% conversion at 130 °C for 24 h) under base. It can be concluded that the presence of base is critical to achieve a high conversion of glycerol under higher temperature or longer reaction time. However, the use of base led to the formation of salts instead of LA and required acidic treatment to isolate LA. Therefore, production of LA from glycerol oxidation under base-free conditions remains highly desirable. Unfortunately, only scarce studies have succeeded in the chemocatalytic production of LA from glycerol without adding base under mild conditions^{23,24}. Liu *et al.* reported that glycerol could be selectively converted to LA by Au-Pd/TiO₂ combined with the Lewis acid AlCl₃ with 100% conversion and 47.6% selectivity at 160 °C for 2 h²⁴. However, dissociation of AlCl₃ and poisoning by Cl⁻ remained issues in such a catalytic process. Fan *et al.* synthesized Pt/Sn-MFI as a heterogeneous catalyst giving 89.8% conversion of glycerol and 80.5% selectivity at 100 °C for 24 h with TOF 1.95²³, but they faced the problem of leaching of Lewis acidic sites Sn from loadings. Most recently, M. Hara's group reported combined Pt/TiO₂ could catalyze one-pot conversion of glycerol to LA with 63% yield and 99% conversion at 150 °C for 18 h²⁵. The above reports pointed that Lewis acids played an essential role for LA production, which accelerated the key step of benzilic acid rearrangement or an intramolecular 1,2-hydride shift²⁶. Therefore, much effort has been done to develop active and durable combined catalytic systems of oxidation and heterogeneous Lewis acid catalysts for efficient cascade conversion of glycerol to LA in aqueous media.

Only recently, we found that a simple phosphomolybdic acid (H₃PMo₁₂O₄₀) was highly efficient for cascade conversion of glycerol to LA in water²⁷ giving 90% conversion and 79% yield of LA at 60 °C for 5 h. And we also for the first time found introduction of Lewis metals Al and Cr into H₃PMo₁₂O₄₀ could enhance their redox ability, and hence to promote glycerol conversion directly to LA combined with Lewis acidity. These bifunctional catalysts - strong oxidative ability and Lewis acidity achieved production of LA with 90.5% selectivity at 93.7% conversion under mild reaction conditions²⁸. As continuation of our research work, other Lewis metals could be introduced to H₃PMo₁₂O₄₀ to evaluate their influence on redox ability and catalytic activity. Herein, Ag-exchanged heteropolyacids (HPAs) Ag_xPMo with varying silver contents were designed to prepare and characterize for glycerol conversion under O₂. Silver ions was used as Lewis centers being introduced to H₃PW₁₂O₄₀, which showed higher efficient for glycerol esterification with acetic acid (AcA)²⁹. And the Lewis acidic strength of Ag_xH_{3-x}PW₁₂O₄₀ (x = 1 ~ 3) was controlled by varying the contents of Ag. To the best of our knowledge, there is no report on Lewis center on redox HPAs apart from the only one report of Al or Cr in H₃PMo₁₂O₄₀. Therefore, the systematical research for the influence of Lewis metals on redox ability and catalytic properties are essential not only for glycerol conversion, but also for other oxidative transformation using a cascade strategy based on multifunctional HPA catalysts. Also the pathway of production of LA from glycerol was checked in order to determine the influence of Ag centers on the conversion of glycerol and distribution of products as well. Meanwhile, conversion of crude glycerol from biodiesel production was done to determine the actual application of Ag_xPMo.

Experimental

Material and reagent. All the chemicals were of AR grade, which were obtained commercially and used without further purification. H₃PMo₁₂O₄₀ was synthesized according to the ref. 30.

Instrument. Elemental analysis was carried out using a Leeman Plasma Spec (I) ICP-ES. IR spectroscopy (4000–500 cm⁻¹) was recorded in KBr discs on a Nicolet Magna 560 IR spectrometer. X-ray diffraction (XRD) patterns of the sample were collected on a Japan Rigaku Dmax 2000 X-ray diffractometer with Cu K α radiation ($\lambda = 0.154178$ nm). The measurements were obtained in the step of 0.04° with account time of 0.5 s and in the 2 θ rang of 5–90°. Raman spectroscopy was obtained on a Renishaw-UV-vis Raman System 1000 equipped with a CCD detector at room temperature. The air-cooled frequency doubled Nd-Yag laser operating at 532 nm was employed as the exciting source with a power of 30 MW. SEM micrographs were recorded on a scan electron microscope (XL30 ESEM FEG 25 kV). EDX spectra were obtained using 20 kV primary electron voltages to determine the composition of the samples. Water contact angle (CA) was carried out by the Contact Angle Meter using the droplet profile as a method. The CA was determined using a tangent placed at the intersection of the liquid and solid. A water droplet with a volume of 2 μ L was dispensed by a piezo doser onto each sample disk. The redox potential were tested by cyclic voltammetry (CV) on a CS Corrtest electrochemical workstation equipped with graphite powder (SP) and liquid paraffin (4:1) as electrodes and saturated calomel as reference electrode. Electrochemical measurements were performed with 0.1 M sulfuric acid solution as the supporting electrolyte. The redox potential of Ag_xPMo catalysts were tested using carbon paste electrode. A TOC analyzer (TOC-L CPH, Shimadzu, Japan) were used to monitor TOC values before and after reaction. The thermo gravimetric analyzer (TGA) and differential thermal analysis (DTA) were used to test the stability of catalysts.

Titration was used to evaluate the total acid content of the solids³¹. 0.05 g of Ag_xPMo was suspended in 45 mL acetonitrile and then the mixture was stirred for 3 h. The density of acid sites in the catalysts was measured by titration with a solution of n-butylamine in acetonitrile (0.05 M) using the indicator anthraquinone (pK_a = -8.2). The IR spectra of adsorbed pyridine (Py-IR) helped to measure the acid content and distinguish the properties of acid sites (Lewis or Brønsted). The samples were exposed to the pyridine vapor for 12 h under vacuum (10⁻³ Pa) at 60 °C. The quantification of acidity was calculated by Lambert-Beer equation (1):

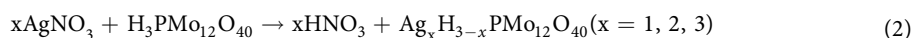
Catalysts	H	P	Mo	Ag	redox potential(V)
HPMo	0.3 (0.2)	1.3 (1.7)	60.0 (63.0)	—	+0.20
Ag ₁ PMo	0.2 (0.1)	1.2 (1.7)	64.2 (59.7)	5.5 (5.6)	+0.63
Ag ₂ PMo	0.1 (0.1)	2.2 (1.5)	54.3 (56.5)	10.2 (10.6)	+0.75
Ag ₃ PMo	—	0.9 (1.4)	48.8 (53.7)	14.4 (15.1)	+0.80

Table 1. Elementary results (calculated values in parenthesis)/wt% and redox potential of different catalysts.

$$A = \frac{\epsilon \cdot w \cdot c}{s} \quad (1)$$

where A is the absorbance (area in cm^{-1}), ϵ is the extinction coefficient (m^2/mol), w is the sample weight (kg), c is the concentration of acid (mol/kg or mmol/g), and s is the sample disk area (m^2), respectively. The amount of Brønsted and Lewis acid sites was estimated from the integrated area of the adsorption bands at 1540 and 1450 cm^{-1} , respectively, using the extinction coefficient values based on the previous report³².

Catalyst preparation. The Ag-exchanged $\text{H}_3\text{PMo}_{12}\text{O}_{40}$ (abbreviated as HPMo) catalysts were synthesized by an ion-exchanged method, according to the procedure described previously^{33,34}. Firstly, 9.125 g (0.005 M) of $\text{H}_3\text{PMo}_{12}\text{O}_{40}$ was dissolved in 20 mL of deionized water at room temperature under vigorous stirring. Then, the appropriate amount of AgNO_3 (0.005 M, 0.01 M and 0.015 M) aqueous solution was added dropwise to the former solution with continuous stirring. A yellow precipitate was formed immediately which was stirred for another 2 h. The large yellow precipitate was filtered and dried in nitrogen. From the TGA and DTA grams (Fig. S1), it can be seen that a decrease in weight up to 250 °C was corresponded to the loss of crystal water molecules in the material. So the yellow powder was calcined at 250 °C in static air for 4 h to loss their crystal water to obtain Ag_xPMo with yield of 78.6%. It also can be seen that Ag_xPMo were stable until 400 °C. The formation of Ag_xPMo reaction undergoes based on the following equations:



Catalytic tests. Glycerol oxidation was performed in a high-pressure batch autoclave of stainless steel with a polytetrafluoroethylene inlet (10 mL). The autoclave was equipped with gas supply system and a magnetic stirrer. A catalyst was suspended in 5 mL aqueous glycerol, and the mixture was heated up to 60 °C. During the reaction, oxygen pressure was maintained at 10 bar. After the experiment, the reaction mixture was diluted 10 times with distilled water and analyzed by high performance liquid chromatography (HPLC) using a Shimadzu LC10A-VP chromatograph equipped with a SPB-10A Variable UV (210 nm) and a RID-10A R.I. detector. Prevail TM C18 column (4.6 mm \times 250 mm) was used with a solution of H_2SO_4 (0.1% w/w) in H_2O /acetonitrile (1/2 v/v) (1.0 mL min^{-1}) as the eluent at 50 °C.

Results and Discussion

Catalyst characterization. To thoroughly recognize the structure transformation induced by silver doping and morphologies of as-prepared Ag-exchanged HPMo catalysts, a combination of elemental analyses, FTIR, Raman, XRD, SEM-EDX, BET and TGA were employed. The elemental analyses of Ag_xPMo were given in Table 1. The results gave the molar ratio of P: Mo = 1:12, showing the formation of dedecomolybdophosphates. The different Ag_xPMo gave Ag: H as 1: 2, 2: 1 and 3: 0, indicating the formation of Ag_1PMo , Ag_2PMo and Ag_3PMo , respectively. Infrared spectra are known to be an informative fingerprint of Keggin structure at molecular level³⁵. FTIR spectra of parent HPMo and Ag_xPMo were given in Fig. 1. In the case of parent HPMo, the characteristic bands of typical Keggin anion can be clearly observed as follows: 1060 cm^{-1} (ν_{as} P-O), 965 cm^{-1} (ν_{as} Mo = O), 882 cm^{-1} (ν_{as} Mo-O-Mo inter-octahedral), and 748 cm^{-1} (ν_{as} Mo-O-Mo intra-octahedral)³⁶, respectively. All silver-exchanged HPMo catalysts exhibited these typical bands at similar frequencies, close to those of parent HPMo, indicating the whole retention of Keggin structure on the as-prepared Ag-salt catalysts. In addition, the shifts of ν_{as} Mo = O occurred from 965 cm^{-1} of HPMo to 942 cm^{-1} corresponding to Ag_1PMo , Ag_2PMo , and Ag_3PMo , respectively. This was proposed to be the interaction between Ag and terminal oxygen of Mo = O leading to some blue shifts of the IR band of ν_{as} Mo = O, which was the main contribution to acceleration of electron transferring in oxidation³⁷. Such blue shifts were correlative to the amount of Ag with the order of Ag_3PMo (23 cm^{-1}) > Ag_2PMo (21 cm^{-1}) > Ag_1PMo (15 cm^{-1}). This result also demonstrated that introduction of Lewis metal ions to HPAs could influence their electron transferring in oxidative reactions. The different redox potentials of as-prepared samples demonstrated this phenomenon (Table 1). As the increase of Ag amount, the redox potential increased from +0.63 V to +0.80 V corresponding to Ag_1PMo , Ag_2PMo and Ag_3PMo , respectively.

Raman spectroscopy is uniquely suited for checking Keggin structure of HPAs to verify the presence and integrity of HPAs structure. Figure 2 showed Raman spectra of parent HPMo and its Ag-salt catalysts. It was identified and attributed Raman bands at 995 cm^{-1} and a shoulder at 965 cm^{-1} to the symmetric and asymmetric stretching modes of Mo = O³⁶. The bands at 850 and 620 cm^{-1} were ascribed to the bending modes of Mo-O-Mo and O-P-O, respectively³⁶. These bands were all clearly identified in the as-prepared silver-exchanged

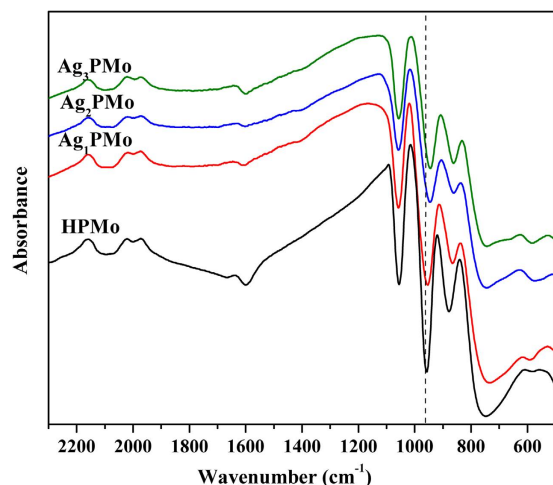


Figure 1. FTIR spectra of bulk HPMo and Ag-salt catalysts.

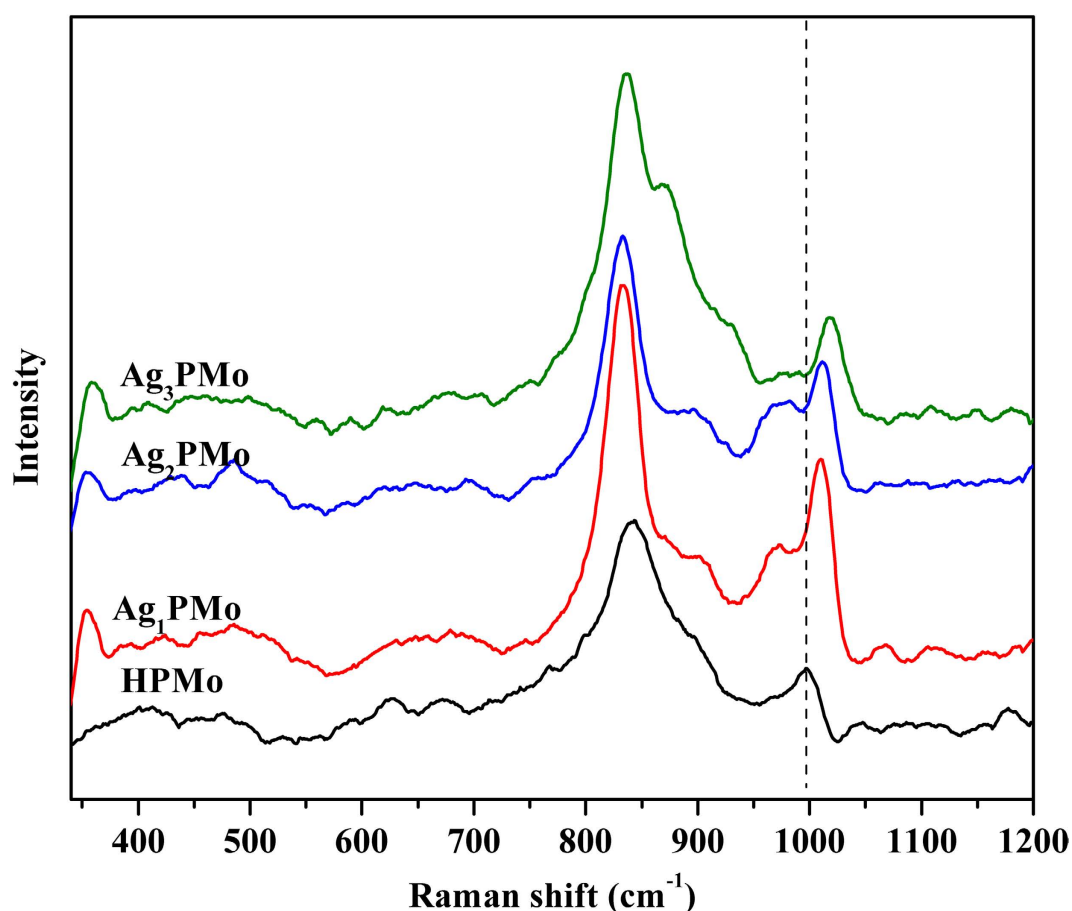


Figure 2. Raman spectra of bulk HPMo and Ag-salt catalysts.

HPMo catalysts, suggesting that the Keggin structure was intact even after exchange of acidic protons with silver. Moreover, about 23 cm^{-1} shift also indicated the linkage between Ag and terminal oxygen.

Figure 3 gave the XRD patterns of parent HPMo and Ag-salt catalysts. The parent HPMo exhibited all of typical X-ray diffractograms of body-centered cubic secondary structure of Keggin anion, with characteristic diffraction peaks at 8.5 , 10.3 , 25.8 and 34.6° ³⁸, respectively. Although the as-prepared Ag-salt samples exhibited very similar diffraction patterns as that of HPMo, a slight shift toward higher 2θ values was observed, suggesting the presence of Ag_xPMo . A detailed study of the predominant 25.0 – 27.0° reflections confirmed this effect, showing the continuous shift toward lower lattice parameters with the increase in silver content, as reported

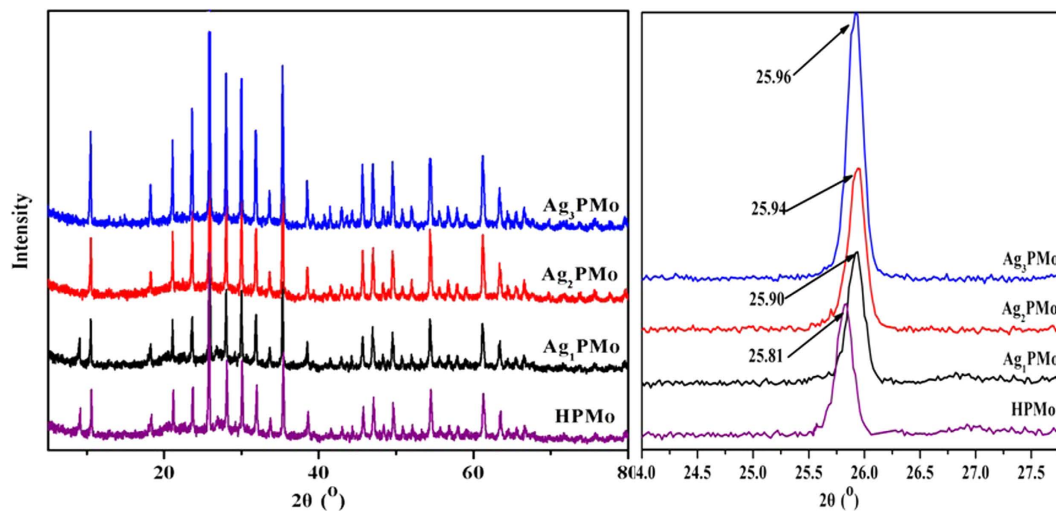


Figure 3. XRD patterns of bulk HPMo and Ag-salt catalysts.

previously³⁹. It is speculated that silver-exchanged HPMo catalysts possess the same symmetry as parent HPMo but with a contracted unit cell. This contraction of unit cell can be explained by the exchange of protons present in the secondary Keggin structure in the form of hydronium ions H_3O^+ for hydrated silver cation (Fig. S2). The same behavior was observed by Borghese *et al.* in the case of silver-exchanged silicotungstic acids catalysts^{33,34}. Accordingly, our XRD patterns revealed the successful incorporation of Ag^+ into HPMo anion with the remaining of Keggin structure.

To gain further insights, SEM was conducted to directly image the as-prepared catalysts. A representative selection of SEM images of Ag_1PMo , Ag_2PMo and Ag_3PMo samples were presented in Fig. 4. It can be found that these as-synthesized materials displayed well-shaped crystalline particles, particularly for the fully substituted Ag_3PMo . With the increase in Ag content, the size of crystalline particles evidently grew, which was because of the replacement of H^+ (with a smaller ionic radius) by Ag^+ (with a bigger ionic radius) as the demonstration in Fig. S2. Furthermore, EDX was examined to determine the elemental compositions of these samples.

From Fig. S3, it can be seen that Ag_xPMo formed mesopore structure and the pore sizes were 4.42, 4.86, and 4.93 nm corresponding to Ag_1PMo , Ag_2PMo and Ag_3PMo , respectively. Fig. S4 also displayed that the catalysts gathered to form micropores somehow.

For the cascade conversion of glycerol to LA, both the surface acid density and the nature of acid sites play the key roles in determining the catalytic performance. Therefore, FT-IR spectra of pyridine absorption were recorded to probe accessible surface acid sites, which is a powerful tool for identifying the nature of acid sites. As shown in Fig. 5, all the samples presented typical bands corresponding to strong Brønsted acid bound pyridine, at around 1540 and 1639 cm^{-1} ⁴⁰. The bands at around 1450 and 1610 cm^{-1} were assigned to the coordinated pyridine adsorbed on Lewis acid sites, while the band at 1489 cm^{-1} was originated from the combination of pyridine on both Brønsted and Lewis acid sites⁴¹. The concentrations of Brønsted acid and Lewis acid sites were obtained from the bands at 1540 and 1450 cm^{-1} based on Lambert-Beer equation, and the calculated results were listed in Table 2. In comparison with pure Brønsted acid of parent HPMo, Lewis acid sites emerged as a result of the exchange of Ag with protons of HPMo, originating from the coordinately unsaturated Ag species in the catalyst. Among them, the Ag_1PMo presented the maximum acidity, even more than the parent HPMo, owing to the enhanced Lewis acid sites. In comparison with the fully Ag-exchanged HPMo sample, partially Ag substituted HPMo catalyst increased available acid sites, due to the presence of residual protons capable of mobility and inducing new strong acid sites³⁵. Similar behavior has been reported in the cases of Cs^+ and Sn-exchanged HPW catalysts^{35,42}. It was interesting to find that the fully Ag-exchanged HPMo sample presented 0.08 mmol/g Brønsted acids, which may originate from the adsorbed surface OH groups or even remaining trace protons. Totally, the molar ratio between Brønsted acid and Lewis acid were 0.86, 0.87, and 0.96 corresponding to Ag_1PMo , Ag_2PMo , and Ag_3PMo , respectively.

Measurement of water contact angle is the most common method for determining hydrophobic property of materials. From Fig. 6, it can be seen that the water contact angle values of Ag_xPMo increased as the growth of Ag number as 90.1 ± 0.3 , 92.3 ± 0.5 and $97.1 \pm 0.8^\circ$ corresponding to Ag_1PMo , Ag_2PMo and Ag_3PMo , respectively, indicating that they all exhibited hydrophobic property compared to their parent $H_3PMo_{12}O_{40}$, which gave a water contact angle of only $26.3 \pm 0.5^\circ$. The hydrophobic property of Ag_xPMo was resulted from the introduction of Ag ion to $H_3PMo_{12}O_{40}$ and the decrease of proton numbers.

Catalytic activity of various catalysts and reaction pathways. The conversion of glycerol to LA reportedly is atom-economic but requires both redox conversion and dehydration/rehydration steps in the presence of a base or Lewis acidic catalysts²⁴, which needs cascade catalysts. Side reactions, such as C–C cleavage, over-oxidation, and over-reduction, must be minimized to obtain the highest yield of LA, which is difficult to be controlled with catalysts operated under harsh reaction conditions. Therefore, to escape over-oxidation, middle oxidative ability of a catalyst is essential for glycerol to LA. In order to evaluate the effect of redox

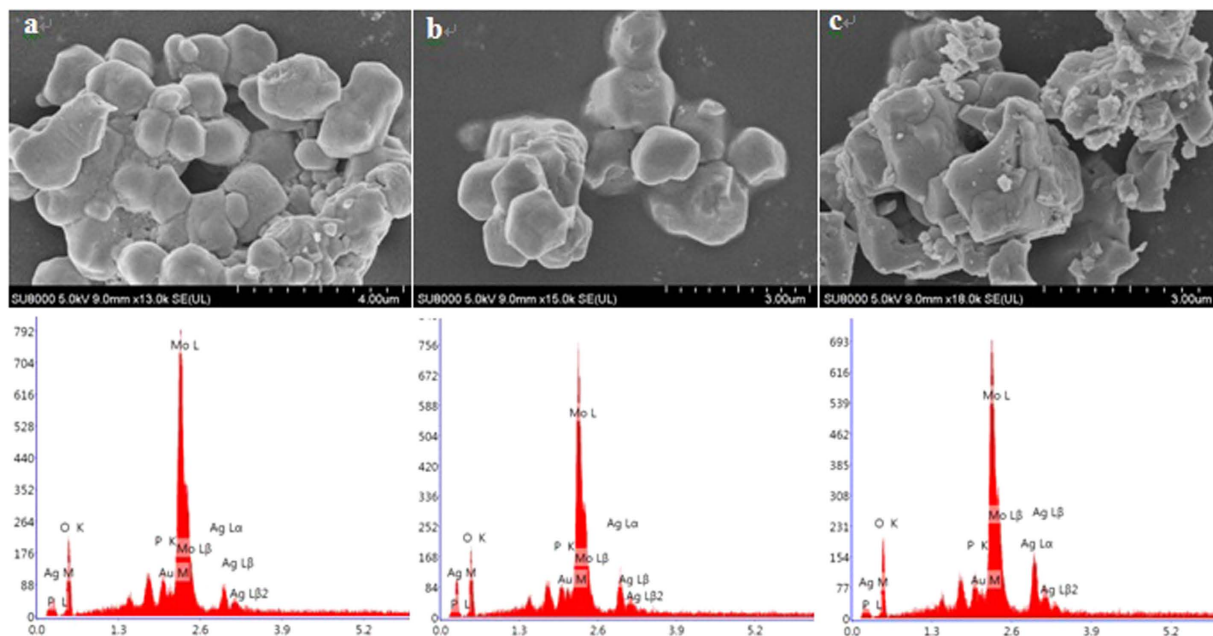


Figure 4. SEM micrographs and EDX of (a) Ag₁PMo, (b) Ag₂PMo, and (c) Ag₃PMo catalysts.

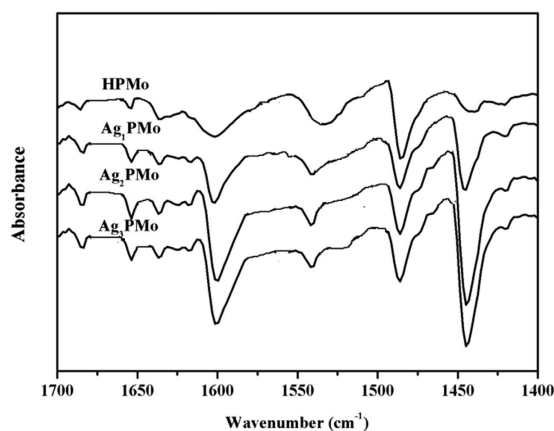


Figure 5. FTIR spectra of pyridine adsorption of bulk HPMo and Ag-salt catalysts.

Catalysts	Bronsted acidity (mmol/g)	Lewis acidity (mmol/g)	Total acidity (mmol/g)
HPMo	1.01	0.03	1.04
Ag ₁ PMo	0.54	0.69	1.23
Ag ₂ PMo	0.25	0.76	1.01
Ag ₃ PMo	0.08	0.86	0.94

Table 2. Amount of acid sites on bulk HPMo and Ag-salt catalysts determined by FT-IR spectra of pyridine absorption.

property on glycerol conversion, a number of phosphorus HPAs were selected including HPMo, H₄SiMo₁₂O₄₀, H₄SiW₁₂O₄₀, H₃PW₁₂O₄₀, H₅PMo₁₀V₂O₄₀, K₃PMo₁₂O₄₀, Ag₁PMo, Ag₂PMo, and Ag₃PMo (Table 3). For free proton HPAs, the conversion of glycerol was in the following order: H₅PMo₁₀V₂O₄₀ (90%) > H₃PMo₁₂O₄₀ (83%) > H₄SiMo₁₂O₄₀ (75%) > H₄SiW₁₂O₄₀ (68%) > H₃PW₁₂O₄₀ (65%). H₅PMo₁₀V₂O₄₀ exhibited the highest activity, whereas H₃PW₁₂O₄₀ was least active. The order of redox potentials were measured as H₅PMo₁₀V₂O₄₀ (+0.93 V) > H₃PMo₁₂O₄₀ (+0.22 V) > H₄SiMo₁₂O₄₀ (−0.39 V) > H₄SiW₁₂O₄₀ (−0.46 V) > H₃PW₁₂O₄₀ (−0.69 V). It is well known that for conversion of glycerol to LA, the first step is to oxidize glycerol to DHA or GCA requiring stronger oxidative catalysts. H₅PMo₁₀V₂O₄₀ exhibited the highest redox ability resulting in highest conversion of glycerol. H₄SiW₁₂O₄₀ and H₃PW₁₂O₄₀ exhibited too low oxidation properties to oxidize glycerol. As for the yields of LA, the

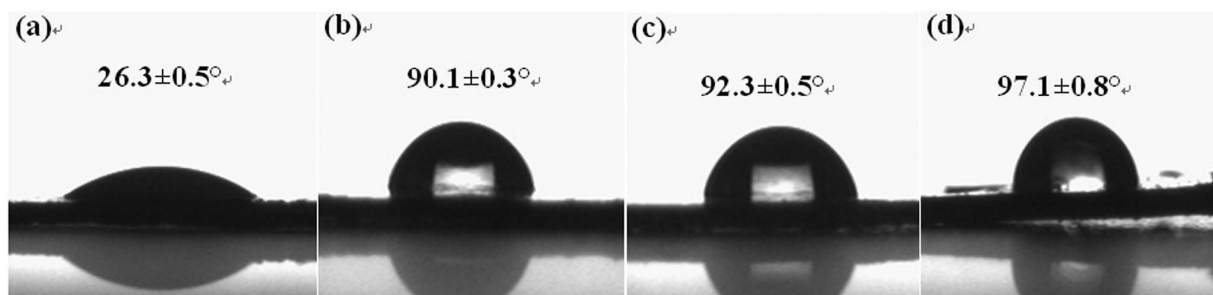


Figure 6. The CA of the two surfaces of HPMo (a), Ag₁PMo (b), Ag₂PMo (c), and Ag₃PMo (d).

Entry	Catalyst	Substrate	TOF, h ^{-1b}	CON, % ^a	Yield LA, %	Selectivity (%)					
						DHA	GCA	PA	LA	GlyA	AcA
1	Blank	Glycerol	0	7	0	58	42	0	0	0	0
2	H ₅ PMo ₁₀ V ₂ O ₄₀	Glycerol	16	90	33	6	5	4	37	23	25
3	H ₄ SiMo ₁₂ O ₄₀	Glycerol	24	75	50	8	7	10	67	4	4
4	H ₄ SiW ₁₂ O ₄₀	Glycerol	20	68	41	13	11	9	60	3	4
5	H ₃ PMo ₁₂ O ₄₀	Glycerol	30	83	60	3	3	13	72	4	5
6	H ₃ PW ₁₂ O ₄₀	Glycerol	19	65	38	19	15	6	58	1	1
7	K ₃ PMo ₁₂ O ₄₀	Glycerol	19	70	39	12	11	12	56	4	5
8	Ag ₃ PMo ₁₂ O ₄₀	Glycerol	35	89	72	6	2	1	81	3	7
9	Ag ₂ HPMo ₁₂ O ₄₀	Glycerol	33	87	68	5	3	4	78	3	7
10	Ag ₁ H ₂ PMo ₁₂ O ₄₀	Glycerol	32	85	64	5	3	6	75	4	7
11	Ag ₃ PMo ₁₂ O ₄₀ ^c	DHA	46	76	59	—	—	12	78	2	8
12	Ag ₂ H ₁ PMo ₁₂ O ₄₀ ^c	DHA	35	70	45	—	—	31	64	1	4
13	Ag ₁ H ₂ PMo ₁₂ O ₄₀ ^c	DHA	27	62	35	—	—	40	56	1	3
14	H ₃ PMo ₁₂ O ₄₀ ^c	DHA	13	40	17	—	—	54	42	1	3
15	Ag ₃ PMo ₁₂ O ₄₀ ^d	GCA	19	52	24	—	—	42	46	9	3
16	Ag ₂ H ₁ PMo ₁₂ O ₄₀ ^d	GCA	16	48	20	—	—	45	42	10	3
17	Ag ₁ H ₂ PMo ₁₂ O ₄₀ ^d	GCA	12	40	15	—	—	50	38	10	2
18	H ₃ PMo ₁₂ O ₄₀ ^d	GCA	7	28	9	—	—	56	32	10	2
19	Ag ₃ PMo ₁₂ O ₄₀ ^e	LA	2	3	—	—	—	—	—	—	47
20	Ag ₂ H ₁ PMo ₁₂ O ₄₀ ^e	LA	4	5	—	—	—	—	—	—	51
21	Ag ₁ H ₂ PMo ₁₂ O ₄₀ ^e	LA	6	8	—	—	—	—	—	—	55
22	H ₃ PMo ₁₂ O ₄₀ ^e	LA	9	18	—	—	—	—	—	—	60

Table 3. Oxidation of glycerol in the presence of various HPA catalysts. ^aCON denotes conversion.

^bTOF = (concentration of formed LA, mol L⁻¹)/((amount used HPA, mol L⁻¹) × (reaction time, h)). Reaction conditions: 5 mL of 10 wt% aqueous solution of glycerol, 0.023 mmol catalyst, 60 °C, 5 h, 5 bar O₂, 800 rpm.

^cDHA as the substrate with the same reaction except the time was 3 h. ^dGCA as the substrate with the same reaction except the time was 3 h. ^eLA as the substrate with the same reaction except the time was 2 h.

range was opposite to active order as H₃PMo₁₂O₄₀ (60%) > H₄SiMo₁₂O₄₀ (50%) > H₄SiW₁₂O₄₀ (41%) > H₃PW₁₂O₄₀ (38%) > H₅PMo₁₀V₂O₄₀ (33%), showing that the catalyst with too high redox potential could not give the highest yield of LA because of the further oxidation. H₅PMo₁₀V₂O₄₀ gave much higher amount of GlyA and over oxidized product AcA due to its high oxidative ability. In order to obtain highest efficiency for glycerol to LA, HPMo was optimized as an available catalyst with middle oxidation-reduction potential. However, H₃PMo₁₂O₄₀ is a homogeneous catalyst in water system that faces the problem of separation and unsatisfactory glycerol conversion.

For phosphomolybdates, Ag₃PMo exhibited the highest activity with glycerol conversion up to 89% under reaction conditions as 5 mL of glycerol solution (1.1 M), 2.3 × 10⁻⁵ mol of catalyst, using 5 bar O₂ at 60 °C for 5 h. The conversion range was Ag₃PMo > Ag₂PMo > Ag₁PMo > HPMo > K₃PMo₁₂O₄₀. As-prepared Ag-salt catalysts presented an enhanced activity for glycerol oxidation compared to their parent and heterogeneous K₃PMo₁₂O₄₀. K ion is a metal ion without any Lewis acidity and did not have positive effect for acceleration the reaction rate. Apparently, the greatly improved catalytic activity of HPMo by adding Lewis metal ions can be attributed to the synergistic effect between the PMo₁₂O₄₀³⁺ and the Lewis acid in oxygenation. Notably, the added metal ions with Lewis acidity having a higher positive charge demonstrated a better efficiency in promoting the catalytic efficiency of PMo₁₂O₄₀³⁺. This effect was attributed to the introduction of Lewis metal ions Ag resulting in shifts 0.43, 0.55, 0.60 V to the positive direction (Fig. S5) corresponding to Ag₁, Ag₂ and Ag₃, respectively, as compared to that of K₃PMo₁₂O₄₀ (0.15 V). Moreover, as demonstrated in Fig. 7, increasing the ratio of Lewis acid/PMo₁₂O₄₀³⁺ would

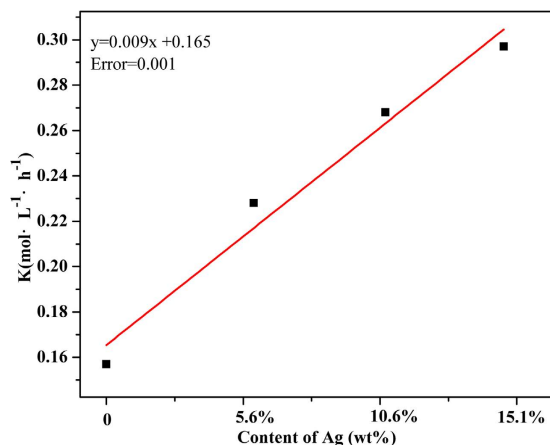


Figure 7. Influence of Ag⁺ concentration on glycerol oxygenation by AgPMo catalysts. Conditions: 5 mL, 1.1 M of glycerol, 2.3×10^{-5} mol of AgPMo, 5 bar O₂, 800 rpm, 2 h.

further accelerate the oxygenation rate of glycerol oxidation. In absence of Lewis metal, the k (rate constant) value for glycerol oxidation by K₃PMo₁₂O₄₀ was 0.157 mol·L⁻¹·h⁻¹, while they were 0.228, 0.268, 0.297 mol·L⁻¹·h⁻¹ in the presence of Ag₁, Ag₂ and Ag₃, representing 1.5, 1.7, 2.0 fold oxidative rate increase, respectively. For LA yields, Ag_xPMo present increasing LA yields from 39% over H₃PMo₁₂O₄₀ to 64, 68 and 72%, respectively. In addition, the TOF (TOF = (concentration of formed LA, mol L⁻¹)/((amount of HPA, mol L⁻¹) × (reaction time, h)) of Ag_xPMo was given with the order of Ag₃PMo (35 h⁻¹) > Ag₂PMo (33 h⁻¹) ~ Ag₁PMo (32 h⁻¹) > HPMo (30 h⁻¹). Meanwhile, the total organic carbon (TOC) before and after glycerol oxidation were 39.0 mg/mL and 38.6 mg/mL, respectively. It can be concluded that no gases were formed during the reaction, showing that glycerol was converted into LA with high selectivity. The enhanced LA yields over Ag_xPMo were also contributed to slow further oxidation of LA to AcA (Table 3, entry 19–22) in comparison to H₃PMo₁₂O₄₀.

Figure 8 gave glycerol conversion and the representative product distributions verse reaction time catalyzed by HPMo and Ag_xPMo. It can be found that (1) as expected, the glycerol conversion increased with the reaction time. And the predominant product of glycerol oxidation catalyzed by HPAs was LA accompanied by DHA, GCA, PAL, GlyA, and AcA. Therefore, it can be proposed that oxidation of glycerol to LA undergoes three steps: firstly, glycerol is oxidized to DHA and GCA; then, dehydration of DHA and GCA gives rise to PAL; and the last step is the benzylic acid rearrangement-like transformation of PAL to LA. (2) For HPMo (Fig. 8a), the formation of GCA and DHA was in equilibrium suggesting that Brønsted acid had no selectivity to the intermediate products. But, oxidation of glycerol over Ag_xPMo (Fig. 8b–d) produced much more DHA than GCA, while increasing the number of Ag gave rise to much more DHA. It is plausible to believe that HPAs with Lewis acidity might be more selective for catalyzing the oxidation of secondary hydroxyl group of glycerol to yield DHA. This is consistent with our observation that DHA led to higher yields of LA than GCA when used as starting materials (Table 3, entry 11–18). And much more Ag in HPAs gave rise to less yield of GCA. (3) The formation of GCA and DHA reached maximum value at a reaction time of 3.5 h then further increasing reaction time did not increase their summed yields over HPMo, while it needed 2.5 h over Ag_xPMo. This might be attributed to the different redox potentials for HPMo and Ag_xPMo as above discussion. (4) At 3.5 h, the summed yield for the intermediates DHA + GCA was 16.1%, whereas the maximum yield to intermediates did not exceed 27.8% in the presence of Ag_xPMo at 2.5 h. HPMo demonstrated lower activity in dehydration of DHA and GCA intermediates to PAL compared to Ag_xPMo. Therefore, the fast transformation of DHA and GCA to LA catalyzed by Ag_xPMo might further impel the glycerol conversion. Therefore, the formation of PAL mainly depended on Lewis acidity^{43,44}. Another proposed reason was due to the relative hydrophobic surface of the Ag_xPMo compared to hydrophilic surface of HPMo. Insoluble Ag_xPMo salts are highly water-tolerant and capable of rapidly releasing of generated water from their secondary structure to promote the dehydration of DHA to PAL. The more water-tolerance is, the rapid speed of generation of LA is. Therefore, Ag₃PMo presented the highest yield of LA under the same reaction conditions. (5) The yields of PAL were lower but the yields of LA were higher catalyzed by Ag_xPMo than by HPMo. Thus, Ag cation with a Lewis acid site had a positive effect on activity and chemoselectivity and played a key role in the reaction pathways leading to LA. In order to test this hypothesis, the compared performance of HPMo for the conversion of DHA to LA was evaluated. From Table 3 (entry 11–18), it can be seen that dehydration rates of DHA or GCA catalyzed by HPMo were slower than by Ag_xPMo. (6) The influence of Ag amount on the conversion of DHA to LA (entry 11–14) was that higher amount of Ag gave higher efficiency from DHA to LA. This further demonstrated the influence of Lewis sites on glycerol conversion to LA. (7) The higher yield of LA over Ag_xPMo was contributed to the less further oxidation to pyruvic acid or AcA (Table 3, entry 19–22). The reason why undesired cascade oxidation of LA was hindered was their unique surface characteristics — the hydrophobic surface. As soon as LA formed, the hydrophobic Ag_xPMo expelled LA molecules from their catalytic sites diffusing to the liquid phase and further oxidation was avoided. H₃PMo₁₂O₄₀ has no such property and LA molecules were prone to be oxidized.

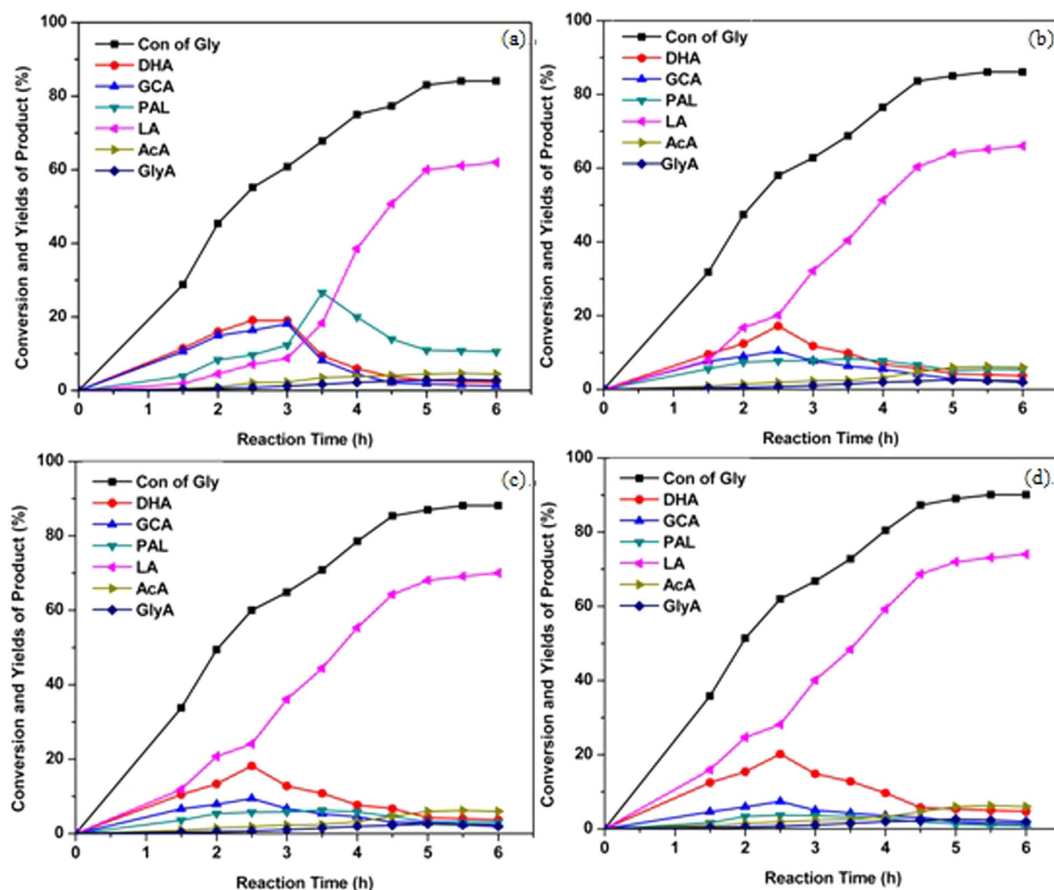


Figure 8. Time course of glycerol and the products. (a) HPMo, (b) Ag₁PMo, (c) Ag₂PMo, (d) Ag₃PMo. Reaction conditions: 5 mL, 1.1 M of glycerol, 2.3×10^{-5} mol of MPMo, 5 bar O₂, 800 rpm.

Based on the above results, we proposed the effect of different catalytic sites on each pathway leading to LA from glycerol (Fig. 9). It can be concluded that optimized redox $\text{PMo}_{12}\text{O}_{40}^{3-}$ center is mainly responsible for glycerol oxidation to DHA and GCA, while Lewis metal Ag could enhance the redox potentials for HPMo through the interaction between oxygen of $\text{PMo}_{12}\text{O}_{40}^{3-}$ and Ag^+ , hence to promote the oxidation of glycerol. Brønsted acid sites favor for generation equilibrium DHA and GCA, while Lewis acid sites are responsible for the formation of DHA which could be dehydrated to PAL much easily. Then PAL converts into LA faster catalyzed by Lewis acid sites rather than by Brønsted acid sites. Therefore, the highest yield of LA was obtained through the synergistic catalysis between redox $\text{PMo}_{12}\text{O}_{40}^{3-}$ and Lewis center Ag^+ .

The significant activity of Ag_xPMo was also attributed to their absorption of glycerol determined by the IR spectra of as-prepared catalysts adsorption of glycerol (Fig. S6). It can be seen that the peaks at 3258, 1360 and 1108 cm^{-1} were attributed to the stretching vibrations of OH and C=O from glycerol, respectively, showing that some glycerol molecules were absorbed by Ag_xPMo catalysts. Meanwhile, the strength of these peaks increased as the increasing of Ag amounts, which was in agreement with the activities (conversion of glycerol and yield to LA) of Ag_xPMo with various number of Ag.

Optimization of reaction conditions catalyzed by Ag₃PMo. The above results revealed that the best glycerol conversion to LA was achieved by Ag₃PMo. In order to optimize LA production, the different reaction conditions, including temperature, reagent concentrations, amount of catalyst, and reaction time were determined (Fig. S7) under Ag₃PMo catalyzing. As observed, increasing the temperature from 40 to 60 °C led to an increase of conversion from 68 to 99% and also increases of LA selectivity from 64 to 93% at 5 h (Fig. S5a). Ag₃PMo was active even at lower temperature of 40 °C, while the best efficiency was achieved as 98% yield at 100% conversion as increasing reaction time to 24 h. Further enhancement of temperature to 70 °C or 80 °C did not improve the activity significantly only giving decreasing selectivity. To the best of our knowledge, it is the highest yield of LA achieved under such lower temperature by now.

The conversion of glycerol and the selectivity to LA increased considerably as enhancement of catalyst usage from 0.007 to 0.023 mmol, achieving the highest of 99% conversion and 93% selectivity using 0.023 mmol of catalyst (Fig. S7b). Further increasing the amount of Ag₃PMo to 0.039 mmol did not give significant increasing trend for conversion but a little decreasing of LA yield. Thus, the oxidation of glycerol was performed at this Ag₃PMo

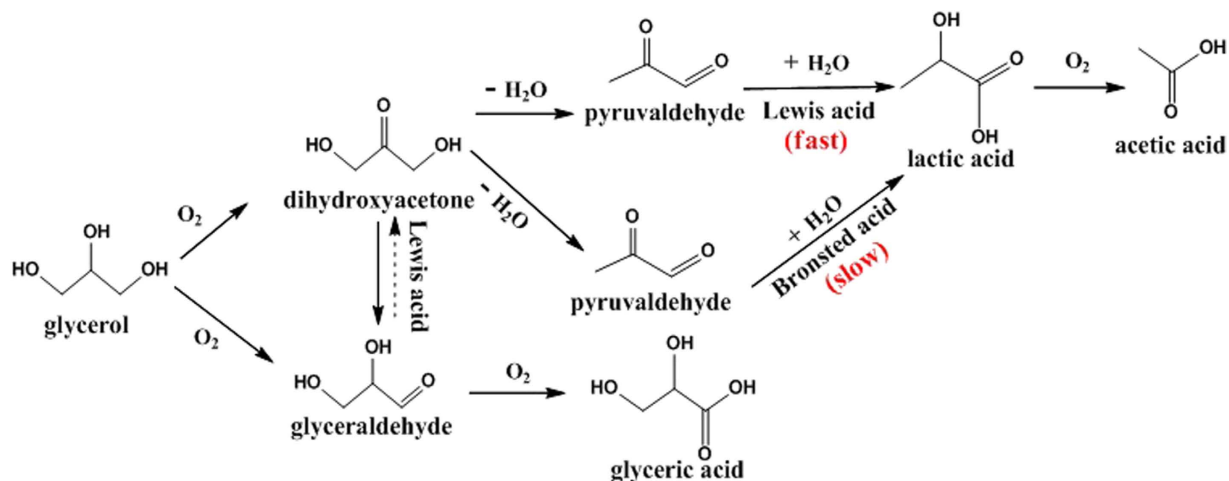


Figure 9. Proposed tandem reaction pathways for the selective oxidation of glycerol to lactic acid over the Ag_3PMo catalysts.

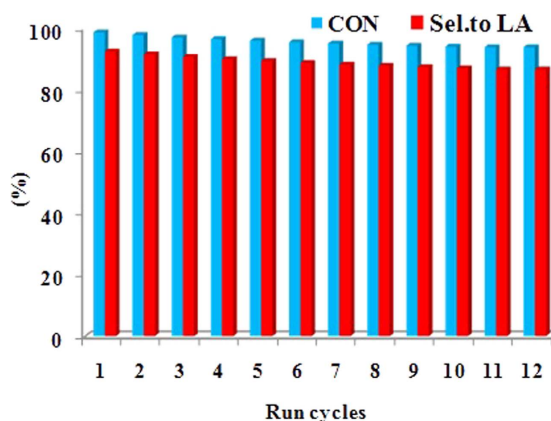


Figure 10. Reusability test catalyzed by Ag_3PMo in oxidation of glycerol. Reaction conditions: 2.3×10^{-5} mol of catalyst, 1.1 M of glycerol (5 mL), 10 bar, 60°C , 5 h.

usage of 0.023 mmol as the molar ratio of glycerol to Ag_3PMo as 239:1, which was comparable to noble metal Pt. And also Ag_3PMo was most active species among solid catalysts even at catalyst loadings as low as 0.02 mmol.

Figure S7c showed the effect of reaction time on glycerol conversion. It suggested that the conversion of glycerol and selectivity to LA increased as long as the time. While after 5 h, there was little change either on conversion or selectivity.

In the investigation of the influence of reagent concentrations (Fig. S7d), the conversion initially increased as the selectivity of LA increased and then decreased as the amount of glycerol increased. This result could be attributed to the increased dihydroxyacetone yield as the amount of glycerol increased, and the dihydroxyacetone required more time to transform to LA. Most importantly, the highest selectivity to LA (93%) was by Ag_3PMo with 1.1 M of glycerol at 60°C for 5 h.

It is interesting to find that Ag_3PMo could successfully catalyze neat glycerol convert to LA under the optimized reaction conditions (5 mL neat glycerol, 0.023 mmol of Ag_3PMo , 10 bar O_2 , 800 rpm, 60°C) with 66% selectivity at 82% conversion for 24 h. This is a very useful result to improve the LA productivities compared to those using low glycerol concentrations.

From Fig. S7e, the conversion of glycerol and yield to LA increased dramatically as increasing the pressure of oxygen, while the selectivity to LA reached 93% with the glycerol conversion of 99% under 10 bar of oxygen. This was attributed to that more oxygen could accelerate the transform from glycerol to DHA in the first step. In view of the economics, air was used to replace oxygen in glycerol oxidation. To our delight, Ag_3PMo showed a decreased but still very satisfactory activity in glycerol conversion into LA with 54% yield to LA at glycerol oxidation of 68% within 20 h.

Reusability of Ag_3PMo catalyst. To assess the reusability of Ag_3PMo catalyst for glycerol oxidation, the spent catalyst was separated from the reaction system by centrifugation after the completion of each run. The spent sample was washed with water, dried at 60°C overnight prior to its reuse for further reaction cycle under the identical reaction conditions. As illustrated in Fig. 10, Ag_3PMo catalyst exhibited similar activity for glycerol

oxidation until 12 reaction cycles without significant loss of its activity. The conversion of glycerol and the yield to LA only decreased 4.8% and 8.9% after twelve cycles compared to the fresh one, respectively. And the total loss of Ag₃PMo was about 5.2% of its initial amount.

In order to determine whether Ag₃PMo leached into mixture or not, the mixture after the reaction was studied by UV-Vis spectroscopy (Fig. S8). It can be seen that there were no characteristic peaks of Ag₃PMo in the range of 200–400 nm, showing no leaching of Ag₃PMo into the reaction mixture. To further determine the leaching of Ag₃PMo, the catalyst was separated after reacting for 2 h (51% of glycerol conversion) and was allowed to react further for over 2 h at the same conditions. The result showed that the conversion of glycerol was only 56.5%, which meant that Ag₃PMo acted as a heterogeneous catalyst without leaching into the reaction mixture during the reaction. The loss of Ag₃PMo was attributed to the operation.

The above results have demonstrated that the Ag₃PMo catalyst is rather durable and holds the potential for practical applications. The excellent reusability of Ag₃PMo was contributed, on the other hand, to its stability during the oxidation reaction, which was determined by IR, XRD, Raman and SEM spectroscopy (Figs S9–12). It can be seen that the spent catalyst displayed similar characteristic bands as the fresh one, revealing that the Keggin structure of Ag_xPMo catalysts remained intact during the reaction. Therefore, Ag_xPMo was rather stable and no leaching under the reaction conditions during the repetitive runs.

Conversion of crude glycerol. Glycerol is a side-product of biodiesel industry with ca. 3×10^6 tons in 2014. Impurity of crude glycerol in quantities makes it difficult to use in most applications⁴⁵. Production of LA from crude glycerol is of great interest and economics, which provides an alternative without any cost of the purification. By now, direct conversion of crude glycerol was via fermentative processes⁴⁶, but only a limited number of microorganisms could be tolerant to complex impurities in the crude mixture. Chemical conversion of crude glycerol is to produce hydrogen and syngas, direct transformation into valued-added products is lacking⁴⁴. There was only one report on chemical transformation of crude glycerol to LA using homogeneous Ir complex as catalyst under alkaline condition with 98% conversion and 96% LA selectivity at 130 °C for 24 h²⁰.

Here used crude glycerol was obtained from biodiesel production without any purification comprising 71 wt% of glycerol, 28 wt % of methanol and other minor organic admixtures. Ag₃PMo was found to be with high efficiency in transformation of crude glycerol with almost the same conversion (98%) and selectivity (92%) under mild conditions (5 mL, 1 M of crude glycerol, 0.023 mmol of Ag₃PMo, 10 bar O₂, 800 rpm, 60 °C, 5 h). This result suggests Ag₃PMo to be a methanol-tolerant catalyst capable of converting crude glycerol. And the esterification of LA with methanol was hindered.

Conclusion

Silver-exchanged phosphomolybdic acid catalysts Ag_xPMo₁₂O₄₀ (x = 1, 2, 3) was prepared and evaluated for conversion of glycerol directly to lactic acid for the first time. It was found that Lewis metal Ag and its amounts could enhance the redox potentials for H₃PMo₁₂O₄₀ to be suitable for oxidation of glycerol to intermediates DHA rather than GCA, while DHA is rather easily dehydrated to PAL than GCA. And then Ag, Lewis center site, favored for further dehydration reaction pathway to LA. Suitable redox potentials, Lewis center sites, and hydrophobic properties render their highly conversion and selectivity. Therefore, a remarkable 93% selectivity to lactic acid at 99% conversion was reached and the undesired cascade oxidation of lactic acid to further AcA was hindered over Ag₃PMo. More importantly, production of LA from glycerol was achieved under mild conditions (60 °C, 5 h), catalyst concentration as low as 0.023 mmol, without adding solvent or alkaline, reusability of Ag₃PMo, and tolerant to crude feedstocks. It fulfills the “green chemistry” concept. To economics and environmental benign, Ag₃PMo as a catalyst for LA synthesis can be highlighted to convert crude glycerol (LA yield 92% under optimized conditions) as well as neat glycerol (LA yield 54% under optimized conditions for 24 h). Stability and no leaching of Ag₃PMo during twelve runs showed that it is rather durable and holds the potential for practical applications.

This study provides a new alternative chemical transformation of glycerol to value-added chemicals under base free with no alkali. This also provides guidance for HPA application in cascade reactions for other biomass-related transformations or organic synthesis.

References

- Dhakshinamoorthy, A. & Garcia, H. Cascade reactions catalyzed by metal organic frameworks. *ChemSusChem*. **7**, 2392–2410 (2014).
- Corma, A. *et al.* Multifunctional hybrid organic-inorganic catalytic materials with a hierarchical system of well-defined micro- and mesopores. *J Am Chem Soc.* **32**, 15011–15021 (2010).
- Diaz, U. *et al.* Catalysis using multifunctional organosiliceous hybrid materials. *Chem Soc Rev.* **42**, 4083–4097 (2013).
- Merino, E. *et al.* Synthesis of structured porous polymers with acid and basic sites and their catalytic application in cascade-type reactions. *Chem Mater.* **25**, 981–988 (2013).
- Zhou, C. H. *et al.* Chemoselective catalytic conversion of glycerol as a biorenewable source to valuable commodity chemicals. *Chem Soc Rev.* **37**, 527–549 (2008).
- Behr, A. *et al.* Towards resource efficient chemistry: tandem reactions with renewable. *Green Chem.* **16**, 982–1006 (2014).
- Corma, A. *et al.* Chemical routes for the transformation of biomass into chemicals. *Chem. Rev.* **107**, 2411–2502 (2007).
- Katryniok, B. *et al.* Selective catalytic oxidation of glycerol: perspectives for high value chemicals. *Green Chem.* **13**, 1960–1979 (2011).
- Purushothaman, R. K. P. *et al.* Base-free, one-pot chemocatalytic conversion of glycerol to methyl lactate using supported gold catalysts. *ChemSusChem.* **7**, 1140–1147 (2014).
- Katryniok, B. *et al.* Highly efficient catalyst for the decarbonylation of lactic acid to acetaldehyde. *Green Chem.* **12**, 1910–1913 (2010).
- Fan, Y. *et al.* Selective catalysis of lactic acid to produce commodity chemicals. *Catal Rev.* **51**, 293–324 (2009).
- Wee, Y. J. *et al.* Biotechnological production of lactic acid and its recent applications. *Food Technol Biotechnol.* **44**, 163–172 (2006).
- Pereira, C. S. M. *et al.* Ethyl lactate as a solvent: Properties, applications and production processes. *Green Chem.* **13**, 2658–2671 (2011).

14. Abdel-Rahman, M. A. *et al.* Recent advances in lactic acid production by microbial fermentation processes. *Biotechnol Adv.* **31**, 877–902 (2013).
15. Shen, Z. *et al.* Effect of alkaline catalysts on hydrothermal conversion of glycerin into lactic acid. *Ind Eng Chem Res.* **48**, 8920–8925 (2009).
16. Shen, Y. *et al.* Efficient synthesis of lactic acid by aerobic oxidation of glycerol on Au-Pt/TiO₂ catalysts. *Chem Eur J.* **16**, 7368–7371 (2010).
17. Li, Y. *et al.* Ni Promoted Pt and Pd Catalysts for Glycerol Oxidation to Lactic Acid. *CLEAN – Soil, Air, Water.* **42**, 1140–1144 (2014).
18. Zhou, C. H. *et al.* Selective oxidation of biorenewable glycerol with molecular oxygen over Cu-containing layered double hydroxides-based catalysts. *Catal Sci Technol.* **1**, 111–122 (2011).
19. Nakagawa, Y. *et al.* Direct hydrogenolysis of glycerol into 1, 3-propanediol over rhenium-modified iridium catalyst. *J. Catal.* **272**, 191–194 (2010).
20. Sharninghausen, L. S. *et al.* Efficient selective and atom economic catalytic conversion of glycerol to lactic acid. *Nat Commun.* **5** (2014).
21. Morales, M. *et al.* Environmental and economic assessment of lactic acid production from glycerol using cascade bio- and chemocatalysis. *Energy Environ Sci.* **8**, 558–567 (2015).
22. Purushothaman, R. K. P. *et al.* An efficient one pot conversion of glycerol to lactic acid using bimetallic gold-platinum catalysts on a nanocrystalline CeO₂ support. *Appl Catal B: Environ.* **147**, 92–100 (2014).
23. Je Cho, H. *et al.* Base free, one-pot synthesis of lactic acid from glycerol using a bifunctional Pt/Sn-MFI catalyst. *Green Chem.* **16**, 3428–3433 (2014).
24. Xu, J. *et al.* Selective oxidation of glycerol to lactic acid under acidic conditions using AuPd/TiO₂ catalyst. *Green Chem.* **15**, 1520–1525 (2013).
25. Komanoya, T. A combined catalyst of Pt nanoparticles and TiO₂ with water-tolerant Lewis acid sites for one-pot conversion of glycerol to lactic acid. *ChemCatChem.* **8**, 1094–1099 (2016).
26. Dusselier, M. *et al.* Lactic acid as a platform chemical in the biobased economy: the role of chemocatalysis. *Energy Environ. Sci.* **6**, 1415–1442 (2013).
27. Tao, M. *et al.* Heteropolyacid-catalyzed oxidation of glycerol into lactic acid under mild base-free conditions. *ChemSusChem.* **8**, 4195–4201 (2015).
28. Tao, M. *et al.* Lewis-acid-promoted catalytic cascade conversion of glycerol to lactic acid by polyoxometalates. *Chem. Commun.* **52**, 3332–3335 (2016).
29. Zhu, S. *et al.* Design of a highly active silver-exchanged phosphotungstic acid catalyst for glycerol esterification with acetic acid. *J. Catal.* **306**, 155–163 (2013).
30. Chamack, M. *et al.* Cesium salts of tungsten-substituted molybdophosphoric acid immobilized onto platelet mesoporous silica: Efficient catalysts for oxidative desulfurization of dibenzothiophene. *Chem. Eng. J.* **255**, 686–694 (2014).
31. Pizzio, L. R. & Blanco, M. N. A contribution to the physicochemical characterization of nonstoichiometric salts of tungstosilicic acid. *Micropor. Mesopor. Mat.* **103**, 40–47 (2007).
32. Emeis, C. A. Determination of Integrated molar extinction coefficients for infrared absorption bands of pyridine adsorbed on solid acid catalysts. *J. Catal.* **141**, 347–354 (1993).
33. Borghese, S. *et al.* Design of silver(I)-heteropolyacids: toward the molecular control of reactivity in organic chemistry. *Catal. Sci Technol.* **1**, 981–986 (2011).
34. Borghese, S. *et al.* Brønsted acid sites in metal-containing solid acids: from quantification to molecular design of new catalysts/silver(I)-polyoxometalates. *Dalton Trans.* **40**, 1220–1223 (2011).
35. Narasimharao, K. *et al.* Structure–activity relations in Cs-doped heteropolyacid catalysts for biodiesel production. *J. Catal.* **248**, 226–234 (2007).
36. Manivel, A. *et al.* Interfacially synthesized PANi-PMo₁₂ hybrid material for supercapacitor applications. *Bull. Mater. Sci.* **37**, 861–869 (2014).
37. Dong, L. *et al.* Lewis-acid-promoted stoichiometric and catalytic oxidations by manganese complexes having cross-bridged cyclam ligand: A comprehensive study. *Inorg. Chem.* **52**, 5418–5427 (2013).
38. Chen, Q. *et al.* Preparation of Keggin-type phosphomolybdate by a one-step solid-state reaction at room temperature and its application in protein adsorption. *J. Sep. Sci.* **37**, 2716–2723 (2014).
39. Zieba, A. *et al.* Transesterification reaction of triglycerides in the presence of Ag-doped H₃PW₁₂O₄₀. *J. Mol. Catal. A: Chem.* **316**, 30–44 (2010).
40. Kourieh, R. *et al.* Investigation of the WO₃/ZrO₂ surface acidic properties for the aqueous hydrolysis of cellobiose. *Catal Commun.* **19**, 119–126 (2012).
41. Budarin, V. L. *et al.* Tunable mesoporous materials optimised for aqueous phase esterifications. *Green Chem.* **9**, 992–995 (2007).
42. Kumar, C. R. *et al.* Samarium-exchanged heteropoly tungstate: An efficient solid acid catalyst for the synthesis of glycerol carbonate from glycerol and benzylation of anisole. *ChemCatChem.* **4**, 1360–1367 (2012).
43. Morales, M. *et al.* Environmental and economic assessment of lactic acid production from glycerol using cascade bio- and chemocatalysis. *Energy Environ Sci.* **8**, 558–567 (2015).
44. Rasrendra, C. B. B. *et al.* Catalytic conversion of dihydroxyacetone to lactic acid using metal salts in water. *ChemSusChem.* **4**, 768–777 (2011).
45. Yang, F. *et al.* Value-added uses for crude glycerol—a byproduct of biodiesel production. *Biotechnol. Biofuels.* **5**, 13–22 (2012).
46. Chatzifragkou, A. & Papanikolaou, S. Effect of impurities in biodiesel-derived waste glycerol on the performance and feasibility of biotechnological processes. *Appl. Microbiol. Biotechnol.* **95**, 13–27 (2012).

Acknowledgements

This work was supported by the National Natural Science Foundation of China (No. 51578119), the major projects of Jilin Provincial Science and Technology Department (20140204085GX).

Author Contributions

M.T. conducted most experiments with help from D.Z. H.G. provided assistance in imaging and data analysis. G.H. provided the help of samples test by HPLC. X.W. provided scientific guidance. M.T. wrote the manuscript. All authors reviewed the manuscript.

Additional Information

Supplementary information accompanies this paper at <http://www.nature.com/srep>

Competing financial interests: The authors declare no competing financial interests.

How to cite this article: Tao, M. *et al.* Designation of highly efficient catalysts for one pot conversion of glycerol to lactic acid. *Sci. Rep.* **6**, 29840; doi: 10.1038/srep29840 (2016).



This work is licensed under a Creative Commons Attribution 4.0 International License. The images or other third party material in this article are included in the article's Creative Commons license, unless indicated otherwise in the credit line; if the material is not included under the Creative Commons license, users will need to obtain permission from the license holder to reproduce the material. To view a copy of this license, visit <http://creativecommons.org/licenses/by/4.0/>